Hardware-in-the-Loop Simulation, Control, and Validation of Battery Inverter Characteristics Through the IBR Control Hardware

Henrique Magnago and Matt Baker
Typhoon HIL, Inc.

David Nobles, Matt Aubuchon, and Eric Herman
EPC Power Corporation

Scott Manson, Lukas Cevetello, and Fernando Calero
Schweitzer Engineering Laboratories, Inc.

Presented at the
49th Annual Western Protective Relay Conference
Spokane, Washington
October 11–13, 2022

Hardware-in-the-Loop Simulation, Control, and Validation of Battery Inverter Characteristics Through the IBR Control Hardware

Henrique Magnago and Matt Baker, *Typhoon HIL, Inc.*
David Nobles, Matt Aubuchon, and Eric Herman, *EPC Power Corporation*
Scott Manson, Lukas Cevetello, and Fernando Calero, *Schweitzer Engineering Laboratories, Inc.*

***Abstract*—Battery energy storage systems (BESSs) are a subject of frequent discussion in power systems. Inverter behavior during power system faults, control stability characteristics, power sharing, and load acceptance capabilities are among the topics that users and manufacturers often discuss. Testing a BESS using a hardware-in-the-loop (HIL) simulator provides meaningful and actionable results.**

BESSs are designed with power electronic switching devices and have a main controller. The behavior of a BESS is programmed through parameters. The switching signals to the electronic switches are the result of proprietary control algorithms that characterize the behavior of an inverter-based resource (IBR). Users of these IBRs want to understand and test these capabilities without running their tests in the actual installation. Simulations can be trustworthy if IBR controller hardware is included and operating in real time, and can also validate the control and dispatch of the IBRs before being deployed in the field.

This introduction gives a brief overview of BESSs. A simple microgrid modeled in the HIL simulator is used to evaluate the performance of a BESS and the protection and control devices during abnormal power system conditions. The results from testing a BESS using a HIL simulator are presented in this paper, and these results are used to illustrate the value that this type of testing brings to the industry.

I. Background

Inverter-based resources (IBRs) can be grid-following (GFL) or grid-forming (GFM). IBRS, such as photovoltaic (PV) inverters and wind generation, are GFL and are following a strong source (the bulk power system, for example) voltage angle. These IBRs cannot operate independently; that is, they cannot be GFM. A GFM IBR is capable of supporting load on its own. A BESS is an IBR that can support load on its own (GFM), but a BESS can also be purchased as GFL. This paper focuses on BESS IBRs in GFM mode, which is the mode that provides many beneficial behaviors for the protection and control of power systems. Many events [1] [2] [3] [4] show that GFL IBRs are promoting a fragile grid, whereas an equal number of reports indicate that properly configured grid-forming with droop (GFMD) IBRs, when properly tested, configured, and maintained, can provide resiliency [2] [3] [5] [6] [7].

Further obfuscating the problem is a lack of reliable simulation tools in regard to IBRs. For example, fault coordination software do not commonly distinguish between GFL and GFM modes. This is concerning as their behaviors are completely different, as shown in Table I.

TABLE I
CONTRASTING GFL AND GFMD BESSS

	GFL	GFMD
Faulted	Offline, Cessation	Current-Limited Voltage Source*
Steady State	Dispatchable Current Source	Current-Limited Voltage Source

* Limited capability.

IBRs must follow the same testing rules that protection relay system designers have used for generations. Relays are tested after installation and after every settings change. This testing commonly includes current and voltage injection test kits. Every firmware update to an IBR also requires a complete retest of functionality in the field.

IBRs, whether they are BESSs or PV inverters or wind turbines, must abide by common-sense rules, outlined as follows:

1. Inverters must act consistently and predictably during both expected and unexpected conditions.
2. Protective relays maintain the security and dependability of the power system under all conditions; namely, relays protect humans, power system assets, and the environment from damage.
3. For any contradictions between Rules 1 and 2, the relay makes the final decision.

The job of protection engineers has become more complex. Through understanding these IBR systems, protection engineers stand a better chance of success. They cannot focus solely on the behaviors of an IBR. Rather, they must understand the whole IBR system, including the IBR, the power source (e.g., PV, wind, or battery chemistry), the power system assets (e.g., transformers, generators, and cables), and the multifunction digital protective relays.

Hardware-in-the-loop (HIL) testing verifies the performance of a BESS during different power system conditions and contingencies. To ensure accuracy in this endeavor, the engineering team has provided a complete system integration of an IBR system to a HIL. This requires three HIL interfaces: one between the IBR and the difference equation solver (HIL),

another between the IBR and the protection and control system, and another between the multifunction relays and the HIL.

II. Inverter Fundamentals

The literature on inverter fundamentals is extensive. This section discusses some of the considerations about inverters that are important to understand in their application and testing.

A. Physical Characteristics

Switching power electronic converters are used for many different applications and have many architectures [8]. Some of the differentiating characteristics include the converter type (e.g., alternate current [ac] to direct current [dc], dc to dc, single-phase, or three-phase), import and export of real and reactive power, switch type and speed, harmonics and power quality, efficiency, dynamic performance, and environmental ratings (indoor and outdoor). Use cases for grid-scale utility and industrial markets include solar, battery energy storage, fuel cell and electrolyzers, wind power, static volt-ampere reactive (VAR) compensation, uninterruptible power supply (UPS), black start, and gas turbine startup.

Three-phase dc to ac inverters are one type of power electronic switching converter that is commonly used. Typical components of a three-phase inverter topology include semiconductor switches, gate drivers, dc capacitors, a real-time embedded controller, sensors (e.g., current, voltage, and temperature), ac and dc filters, switches or contactors, protection (e.g., breaker, fuse, transient voltage suppressors, surge-protective devices), thermal management (e.g., fans, filters, or heat exchanger), and a structural enclosure.

All of these components have operational limits and constraints that an inverter manufacturer considers when designing an inverter to achieve the desired performance. For example, one type of electronic switch is an insulated-gate bipolar transistor (IGBT). IGBTs have limits, such as maximum voltage, current, switching speeds, losses, heat transfer capability, and lifetime. At higher power and voltage levels, commercially available switch ratings become more discrete and limited. Typical IGBT voltages above 1 kV are 1,200 V, 1,700 V, 2,200 V, and 3,300 V with few or no devices in between, so higher power inverter designs are constrained to use this limited device selection.

Electronic switch types include bipolar junction transistors, IGBTs, field-effect transistors (FETs), and thyristors. Typically, PV and battery energy storage system (BESS) inverters are implemented with IGBTs or FETs, allowing pulse-width modulation (PWM) techniques. There are also several different semiconductor materials available, including silicon, silicon carbide, and aluminum gallium nitride. It is worth noting that silicon IGBTs are typical for about 300 kW to more than 1 MW class grid-scale inverters and that silicon carbide FETs are rapidly maturing in capability. A typical battery inverter design is shown in Fig. 1.

Fig. 1. Modern BESS.

B. Switching

Inverting from dc to ac is accomplished with the fast switching of the dc source. The dc source voltage can be made constant with a parallel capacitor, as shown in Fig. 2, making the inverter a voltage source inverter (VSI), as defined in the industry. The dc source can be made a current source inverter (CSI) with a series inductor, as shown in Fig. 2. BESSs are typically VSIs.

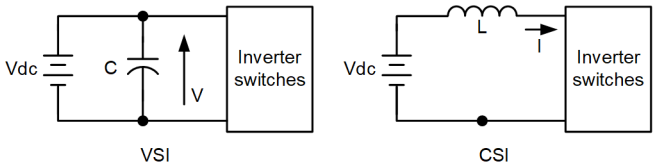

Fig. 2. VSI and CSI.

Fig. 3 is a simplified diagram of a two-level, three-phase inverter. Each phase has two switching devices, an upper and lower switch, referred to as a half bridge. When operating, either the upper switch (S11, for example) or the lower switch (S12) in a half bridge can be on, but not both, as that would cause a short between the dc bus. The half-bridge switches are alternatively switched rapidly, with varying durations, to synthesize a sinusoidal ac voltage waveform with a PWM scheme. The phase voltage is related to the duty cycle of the PWM pattern. A 50 percent duty cycle (in which the upper switch and lower switch are on for equal amounts of time) averages out to zero-output voltage. A longer duty cycle on the upper switch, and hence shorter duty cycle on the lower switch, averages out to a net positive-phase output voltage. The opposite scenario averages out to a negative-phase output voltage. This is the fundamental mechanism for controlling the inverter voltage, current, and power flow.

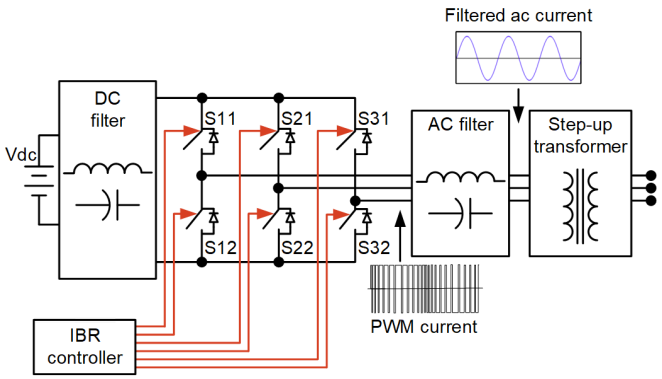

Fig. 3. A 2L inverter with ac and dc filters, showing voltage and current sensor locations, ideal switches with antiparallel diodes, dc bus caps, batteries, and a controller.

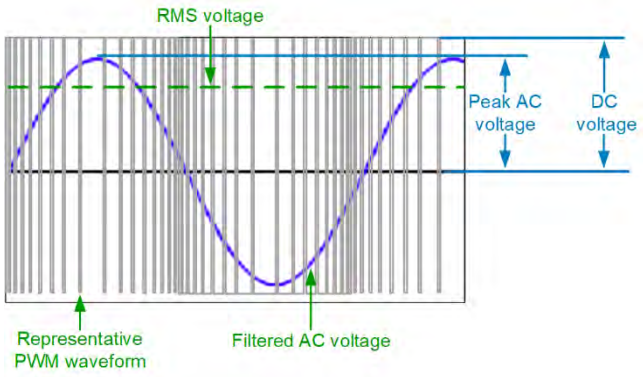

Fig. 4. Representative waveforms of single-phase PWM and filtered ac voltages.

The switching PWM waveform inherently creates a train of pulses, which contains many higher frequency harmonics. An ac filter is typically used to remove the high frequency switching harmonics and present a higher quality sinusoid at the terminals of the inverter. Switching frequencies range between a few kHz to over 100 kHz depending on the switching device characteristics and inverter architecture. Harmonics in this context means harmonics of the switching frequency, not harmonics of the fundamental ac frequency. Since the switching frequency is usually much higher than the fundamental frequency, the ac voltages and currents at the output terminal of the inverter can have very low fundamental harmonic content (5th, 7th, 11th, 13th, etc.). The ac filter also plays an important role in the control of the inverter by providing a small impedance between the half bridges and the grid network, which the inverter controller can leverage to ultimately control the inverter current and power flow. The ac filter, LCL components, and the transformer associated with the inverter do not allow for the propagation of the switching frequency harmonics.

The PWM pattern of one of the phases of a two-level inverter is shown in Fig. 4. The output of the half bridge is either connected to the positive dc bus or the negative dc bus, but not zero or an in-between voltage. This leads to common-mode voltage. For example, if the negative side of the dc bus is chosen to be grounded, the output phase voltages go between ground and the positive dc bus rail. This means that our output voltage ac waveforms have a dc offset. This is the common-mode voltage, the shape of which is dependent on where the ground is connected. It is common to leave the power electronic circuits floating and galvanically isolated or referenced to a virtual midpoint to best manage common-mode voltages. IBR users do not need to be concerned about this common-mode voltage as it is not an issue on the primary side of the transformer associated with the inverter. The IBR designers and any HIL simulation, however, are aware of its presence.

C. *Inverter Considerations*

This common-mode voltage also makes paralleling inverters challenging. If more than one inverter is paralleled with the ac phases connected and dc bus connected, the common-mode voltage can drive common-mode current between the converters, referred to as circulating current. Circulating currents can be challenging to manage when multiple inverters are connected in parallel on the dc side.

Another important note is that the maximum ac line-to-line peak voltage that can be produced is ideally equal to the maximum dc bus voltage when one phase has the upper switch on and another phase has the lower switch on. The dc bus voltage needs to be high enough to support that desired ac voltage. If the dc voltage is too low, the inverter is not able to produce the desired ac voltage.

Also, if connected to a grid, a low dc bus voltage can be driven higher by the passive rectification of the ac voltage through the switches' antiparallel diodes. This is effectively an uncontrolled region of operation, where the higher rectified ac voltage would create an uncontrolled dc charging current into the dc source. Consequences could include overcharged and damaged batteries, blown fuses, and similar undesired situations. Therefore, this region of operation is typically avoided.

Another important consideration for IBR is the abnormal power system faults that occur due to nature or failure of equipment. These are generally short circuits. If there is a short on the grid, the inverter senses and responds quickly by adjusting the PWM waveform to match the low voltage. However, the current that the inverter can produce is typically limited to something close to the nominal rated value. This is because, unlike many rotating machines, the thermal mass of the switches is very small. The actual volume of silicon IGBT producing the waveform is tiny in comparison to a generator winding. A small amount of overcurrent for a short period of time is sometimes acceptable, but high current would quickly damage the IGBTs. Therefore, the short circuit performance of most inverters is close to the rated value. Typical values are 1.1 to 1.2 pu. If more short circuit current is desired for a site or project, it is common to deploy more inverters than is otherwise needed during nominal operation.

D. Low-Level Inverter Control

The low-level control of the inverter is typically accomplished with a real-time embedded processor or digital signal processor (DSP) and may or may not run a real-time operating system (RTOS). Low-level control architecture can vary a lot depending on the inverter features and functions. Some inverters require grid voltage to be present and simply push around real and reactive power. Other inverters regulate voltage and frequency and can also form a grid if desired. There are also numerous grid support functions defined by a variety of standards, such as UL 1741, IEEE 1547, and AS/NZS 4777, that prescribe an inverter's response to potential grid deviations. For example, these grid interactive inverters have tables that an end user can set to provide real power in response to frequency variations (i.e., Hz-watt or frequency watt) to help strengthen the local grid.

Grid-scale utility industrial inverters commonly use standardized communications protocols for command and control from energy management systems or power plant controllers. Physical layer protocols include serial links, Controller Area Network (CAN) buses, and copper or fiber Ethernet. Higher level protocols include Modbus, SunSpec, IEEE 2030.5, and Distributed Network Protocol (DNP3). It is common for inverters to have a combination of these standard protocols that define functions common to all inverters (e.g., enable or disable, inverter status, and real and reactive power command set points) as well as custom communications mappings for additional features unique to that particular inverter.

E. IBR Transformer Connection

As shown in Fig. 3, the three-phase step-up transformer is an important component of a modern IBR. Power electronics cannot easily accommodate medium-voltage or high-voltage (HV) levels, and the voltage needs to be stepped up as with generators.

The low side of the transformer is generally ungrounded Y- or delta-connected. The power electronics (Fig. 3) do not generally have a ground return path as the inverter full bridge is left floating and ungrounded. With no return path, there is no possible 3I0 current. The inverter bridge must be provided with a ground return path if the inverter is specifically designed to produce ground currents and is directly connected to grounded loads (with no step-up transformer).

The high side of the transformer is generally a Y connection. For sensible ground fault protection, 3I0 is expected on this side. If the IBR is the only source on the HV side, the Y side is connected to ground. If there is more than one IBR step-up transformer in parallel, a grounding transformer is preferred to provide the ground path on the HV side of the transformer.

Any negative-sequence components on the low-voltage side are transformed to the HV. Negative-sequence components are not blocked by the step-up transformer. Modern BESSs can produce significant amounts of negative-sequence components when operating in GFM mode.

F. Inverter Real and Reactive Power Capability

The power capability of inverters may vary widely depending on the design constraints and topology. Further, the power capability is dependent on the set point of operation. For example, an inverter operating with 1,000 Vdc may have a wildly different power capability than an inverter operating with 1,200 Vdc. It is difficult, if not impossible, to generalize the power capability of inverters.

However, it is not uncommon for BESS designs to require a converter capable of fully symmetric real and reactive power limits in the desired region of operation. The most common reason for this is that when exporting or importing power to the grid, it is typical to only import or export real power at the point of interconnection. To achieve this, the inverter must account for the reactive power consumed by any transformers in that path. A fully symmetrical power curve provides the largest degree of control. For some BESSs, this full-circle capability may be a requirement of the interconnection agreement.

Fig. 5 illustrates the power capability of a 1.5 MVA inverter, and in this example, it is a full circle. It is also worth noting that as current is often the limiting factor of inverter power capability, it changes as a function of the grid voltage. Therefore, in the following figure, the solid line represents the capability at nominal grid voltage, while the inner circle represents the capability at a low grid voltage and the outer circle represents the capability at high grid voltage.

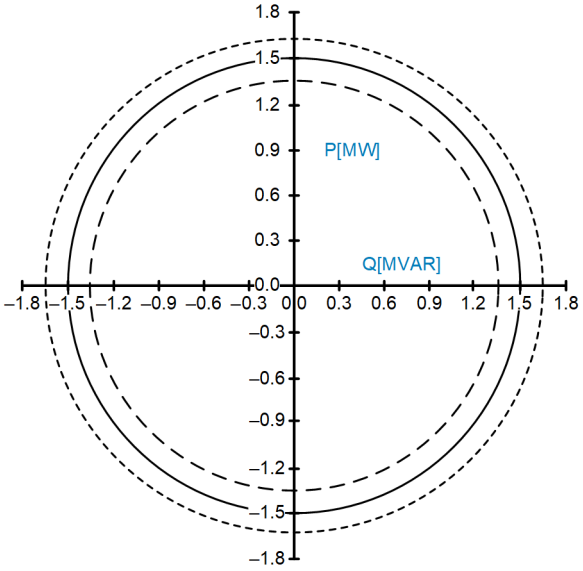

Fig. 5. Ideal inverter capability curve.

G. Final Considerations

In this section, a few of the functionalities in IBRs were briefly mentioned. When looking from the power system side, most of these functionalities are not relevant: the IBR is simply expected to work, regardless of its inner workings. Different IBR manufacturers can implement each of these functionalities and processor arrangements (field-programmable gate array [FPGA], DSP, RTOS, etc.) in a multitude of different ways; hence, every single IBR is unique. The large majority of these differences are present in the IBR's control board and

embedded software, which are the same ones that remain intact on a controller hardware-in-the-loop (CHIL) setup.

Depending on the application, IBRs may go through a certification process [9] so that under normal and steady-state operating conditions, the behavior is known. The same does not hold true for dynamic conditions. Different implementations and designs present different dynamic responses, fault responses, stability, robustness, and overall performance in scenarios with varying parameters. Other factors, such as communications, connectivity aspects, state machines, and procedures, are involved as well.

For these reasons, to capture an accurate response of a power system in a simulation that contains IBRs, the system must have the IBR controller in the loop. Hence, the whole system has to be emulated to the degree of fidelity required by the IBR controller.

III. Control of Inverters

Battery inverters have a source of energy readily available for control. In practice, battery inverter systems are the most appropriate sources to maintain an islanded microgrid or distribution loads [5]. This is because a source can generate and maintain its own voltage and frequency references for supplying loads and other sources when battery inverters are in GFM [6] [7] [10].

Inverters that do not have a dispatchable energy source (PV or wind) are GFL inverters. Inverters with a battery source (BESS) can operate as GFL as well, and they are also capable of being GFM inverters. The GFL mode does not allow the IBR to support an island and requires a strong source for it to be controlled [6] [7] [10]. Moreover, GFL inverters (PV and wind) do not have a large margin of energy stored and are operating at their maximum power point.

A GFL inverter is designed around a synchronization algorithm, in which the voltage frequency and phase angle are computed based on voltage measurements. There are many possible algorithms [11] with different characteristics. Among them, phase-locked loop (PLL) is widely used. The frequency and phase angle are used to define the injected current. Many control schemes can be used to control the output current [12] and the modulation strategy [13]. A simplified GFL control scheme is shown in Fig. 6. The inverter's control is based on Park's dq transform, and this transformation requires the operating frequency, used to yield θ(t), which is derived from the measured ac quantities at the three-phase terminals of the inverter. The inverter control is the proprietary algorithm that implements any support functions related to the operation of the inverter [14]. In Fig. 6, vd and vq are the direct and quadrature Park components after being processed in the inverter control, and mx and sx (where x is a, b, or c) are the modulated and switching signals per phase.

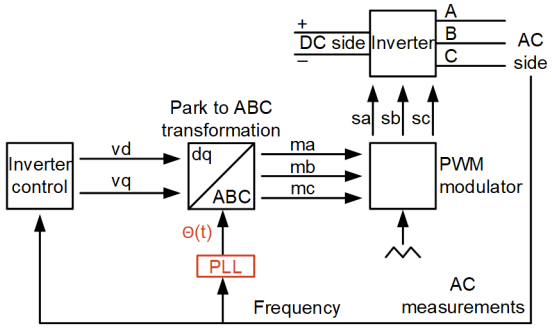

Fig. 6. GFL inverter.

A GFM inverter must not rely on a PLL to provide control. It generates its own angle reference [14]. The measurement of the output power compared to a set power is the main algorithm; based on this difference and other support functions, the inverter controls its output. In Fig. 7, Pmes and Pset are the measured and set-point real power values, respectively.

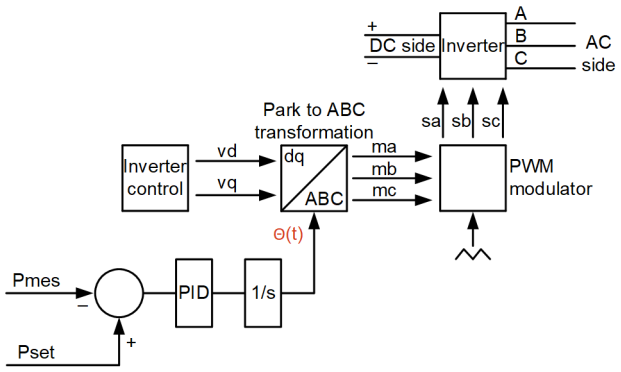

Fig. 7. GFM inverter.

There are certain support functions and methods that can be used to implement a GFM inverter. The one that we focus on in this paper is droop control frequency, in which the inverter implements the droop function typical of synchronous machines.

Fig. 8 illustrates a droop curve that relates the output power to the operating frequency of the inverter. This behavior is that of rotating generators. For a set frequency at no load (60 Hz in the figure), an increase in power represents a proportional decrease in frequency dictated by the droop ratio (4 percent in the figure).

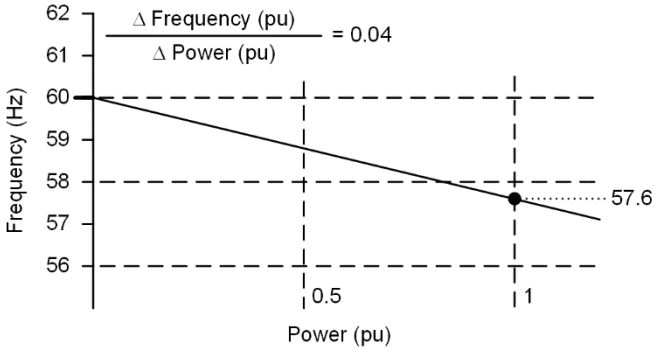

Fig. 8. Power and frequency droop characteristic.

Fig. 9 illustrates the implementation of the droop curve in a GFMD inverter. The measured real power (Pmes) is related to a change in frequency by the droop constant *d*. A proportional integral controller and an integrator (1/s) can be implemented to determine the angular relation to time for Park's transformation.

The GFMD inverter is a type of inverter that is being used extensively for microgrid applications and islanded systems [2] [3] [4]. The droop behavior makes GFMD inverters practical for GFM applications.

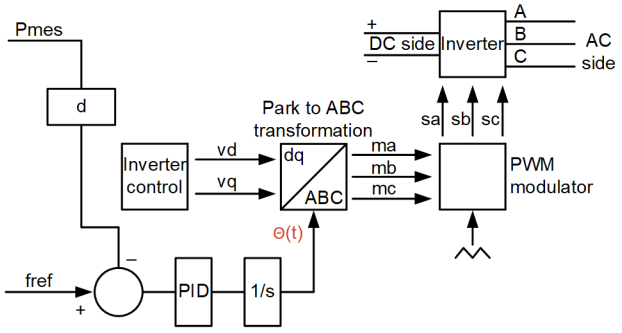

Fig. 9. GFMD inverter.

For decades, rotating machinery controls and mechanical characteristics have shown that a droop characteristic is desirable. Load sharing is inherent in the behavior of the sources. In Fig. 10, the load is shared equally (in percent) by the two sources, even if they are of different sizes. The percentage contribution is the same for both since they have the same droop coefficient (d), and if there is an overload, both sources are overloaded equally. This is a desired characteristic when paralleling sources and sharing loads.

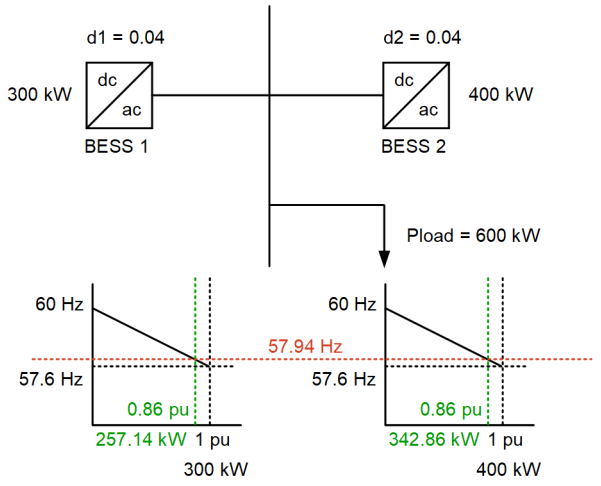

Fig. 10. Load sharing is inherent with droop characteristics.

The frequency behavior of the droop curve in the GFMD inverters allows for the use of similar techniques as in rotating machines. Load shedding can be based on frequency thresholds [2]. For an overload, the system frequency decreases and load-shedding steps can be proposed.

While load sharing in steady-state conditions is straightforward, as shown in Fig. 10, load acceptance transients need to be considered [2] [4]. An inverter can accommodate only some amount of load when a load breaker is suddenly closed and allow the power system to remain stable. GFMD inverters have significant stability to large load acceptance steps, but there is a limit.

The transition from grid-connected to an islanded microgrid requires certain considerations for the operating mode of the islanded battery inverters. There are philosophies that change the mode of these from GFL to GFM, and when grid-connected, back to GFL. This allows for greater precision in the control of P and Q dispatch on a stable grid. This, however, comes at the cost of reduced stability in the event of unintended islanding conditions. The industry suggests GFMD for a seamless operation of battery inverters [5] [10] [15] with no change of operating mode. The GFMD provides the droop characteristics that allow islanded operation and load sharing [16] [17] [18].

As mentioned previously, GFMD inverters are voltage sources, and theoretically, short circuits near the terminals of the inverters should provide significant fault current. Unfortunately, for the protective relays that are provided to detect faults, the short circuit currents of inverters are limited by current limit thresholds in the control algorithm of the inverter. The protective relays, which can be inverter controllers as well [15], provide protective relaying functions that need to be appropriate for the small contribution of fault current from the inverters [5].

IV. HIL Fundamentals

HIL is a development and validation methodology used for decades in safety-critical applications, such as automotive and aerospace. In these fields, HIL testing has become mandatory as one of the steps for certification and approval of new or updated products [9].

HIL solutions model power systems and electrical components within their time frame of interest. For example, the accurate modeling of IBR switching, IBR control loops, transformer core flux calculations, etc., require microsecond time steps for accuracy. Protective relays and control equipment can be simulated with time steps of a few milliseconds. Other slower-reacting devices on generators, like automatic voltage regulators, can be studied with time steps of hundreds of milliseconds.

In the last decade, advancements in the computational power of FPGAs and microprocessors, and new methodologies for real-time simulation allow emulation of the kHz speed switching of IBRs in real time. In this section, we explore some of the characteristics and features of real-time HIL simulators. This solution can be used for any power electronics-based converter, including BESSs, PV inverters, wind power inverters, machine drives, electric vehicles (EV), EV chargers, and active filters. The real-time simulator accurately models the switches (IGBT, FET, etc.) used in IBRs. The IBR controller links to the real-time simulator at the same hardware level that it would be linked to in the actual installation.

A. HIL Simulation Requirements

The goal of CHIL methodology is to model well-known components, such as passive components, cables, machines, and semiconductors with optimal fidelity, and combine this with the real controller, which is a difficult component to model accurately when everything is running in real time. Fig. 11 demonstrates exactly that, where the same controller used in the final product remains, and the rest of the system is modeled and computed in real time. The controller does not distinguish if it is interfacing with the real system or the real-time HIL simulator. The controller sends the gating signals to the HIL, and the HIL computes how the system behaves with such inputs and returns measurements to the controller. This cycle repeats itself every simulation step, generally under 1 µs, currently going as low as 200 ns. This extremely high resolution is required specifically to model both the IBR switching and the particular switching devices used (IGBTs, for example) and enable the use of the real IBR controller but is not necessary for the power system behavior. The IBR controller has full control of the modeled switches; therefore, the IBR is emulated with accuracy. The user can configure the IBR controller parameters as if the IBR were in the field.

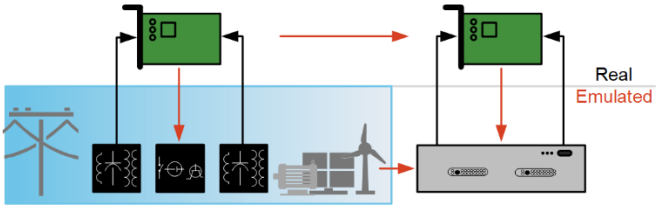

Fig. 11. The CHIL model: the real system is shown on the left. The real controller with the rest of the emulated system is shown on the right.

Another critical time requirement on real-time HIL simulators is the time interval between the samples of the gating signals. This determines the duty cycle of the semiconductors in the simulation, and the gating signals must be sampled in the order of single-digit nanoseconds. IBRs can use switching frequencies in the range of hundreds of kHz, such as EV charging stations, and use PWM signals with high duty cycle precision, hence the need for such a small sampling time interval.

B. Types of Testing

When testing the controller, there is generally a tradeoff between cost and fidelity, with different levels of test coverage. Fig. 12 compares the five most used options.

Most IBR development starts with pure simulation tests, as shown in Fig. 12a, where constraints of the controller hardware are not taken into consideration and different modeling approaches with different fidelities can be used. Another option is software-in-the-loop, shown in Fig. 12b, where both the controller and the rest of the system are still simulated. Now there is a clear separation between the controller and the rest of the system, where it is possible to include certain controller hardware limitations.

The sweet spot between cost and fidelity is CHIL, as shown in Fig. 12c. The lack of the power stage in these methodologies allows a very large number of scenarios to be tested, many of which cannot be performed with full or partial power. With CHIL, everything except the controllers is modeled, hence we model the previously mentioned well-known elements and use the actual controllers, which are not feasible to model with high accuracy for real-time applications. Modern IBRs not only control voltage and current but also have several modes of operation, parameters that can be changed, communications protocols, protection functions, and many more features.

Lastly, we have methodologies that use an IBR's nominal power. Power HIL setups are generally used to validate the power stage, either by using a simpler modeled version of the real controller, as shown in Fig. 12d, or by including the actual controller. This methodology allows for full control of the operating condition of the IBRs, validating both the power stage and IBR controller. A similar approach is used by certification laboratories when testing IBRs. The downside of these approaches is that they add the dynamics and limitation of the power amplifiers and reduce the test coverage, ease of use, and safety, which considerably increases the cost. The last option, shown in Fig. 12e, is running everything with all real devices deployed in the field. In this case, there are no approximations, but many tests cannot be performed. Any misbehavior of the system can cause costly and harmful incidents.

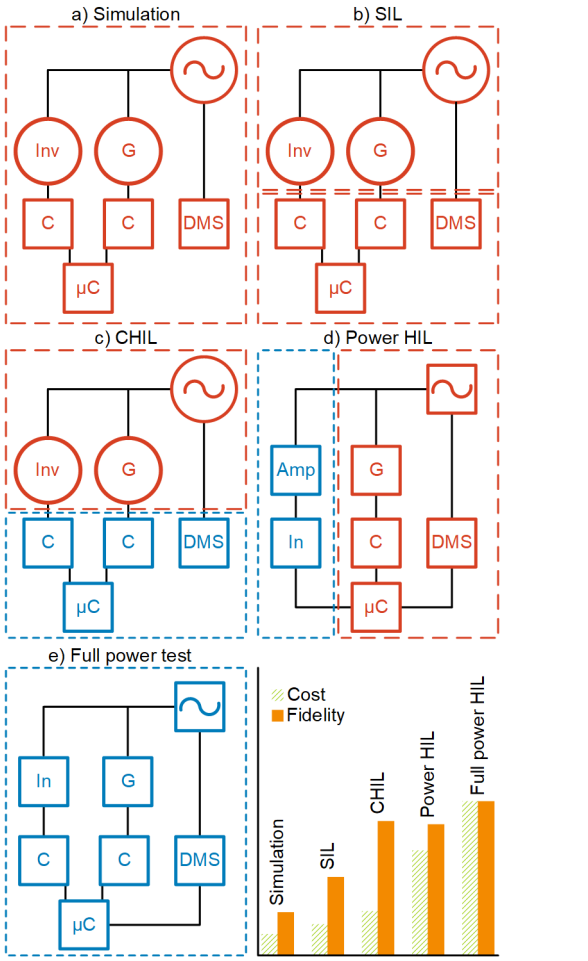

Fig. 12. The red part of the system, which is surrounded by longer dashes, is the part of the system that is modeled. The blue part of the system, which is surrounded by shorter dashes, indicates the part of the system that is real. Different validation options compare the cost and fidelity of each methodology in the graph.

C. CHIL: Interfacing With the IBR Controller

As shown in Fig. 11 and previously mentioned, the HIL simulator should behave like the real system, simulating all the components from the power stage in such a way that the controllers cannot distinguish the real system from the real-time HIL model. IBR controllers are based on microprocessors and interface with the power stage by means of low-voltage digital and analogical signals. The digital gating signals sent from the controller to the gate-driver range from 0 V to 3.3 or 5 V. The voltage and current measurements are converted, if needed, and scaled down to +/– 10 V or 0 V to 3.3 or 5 V. These voltage levels are suitable to be directly connected to most HIL simulators.

When using the low-voltage level interface of protective relays or other power system components, the same holds true. If opting to use the potential transformer and current transformer channels, an amplification (in the case of the voltage) and transducing (in the case of the current) interface board should be used between the HIL and controller. The low-voltage channels from HIL voltage measurements are amplified to adequate voltage levels at very low currents. The low-voltage channels from HIL current measurements are transduced to adequate current levels at low voltages. This means the setup is still low power since voltage and current are amplified separately.

Another key factor for interfacing with several controllers, especially IBRs, is the number of HIL inputs and outputs (I/O). To accurately represent power systems and microgrids, the HIL simulation needs to be comprised of dozens, if not hundreds, of devices. Hence, the option of paralleling HIL devices and/or adding expiation cards is a must to either increase I/O capacity or increase the modeled system complexity.

Since real controllers are used, the communication can happen directly between these devices. If necessary, certain devices can also be completely emulated inside the HIL, including the communications maps and protocols. Hence, the HIL should also provide a wide range of communications channels and protocols.

D. Features of HIL Simulators

HIL technology allows engineers to safely test a wide range of operating conditions using the actual controllers that are implemented in the field. For instance, it can be used to validate the parametrization of each device, show how the IBRs behave when integrated with the rest of the system, and communicate with different devices. Certain features are necessary to allow proper test coverage and validity:

- An efficient and accurate model solver
  - The solver includes models that are designed to be stable and behave as designed in the modeling environment, thus accurately representing the real system if modeled properly.
- Easy-to-use, flexible modeling environment
  - The modeling environment includes a wide library of commonly used inverter topologies, motors, devices, and communications protocols.
  - It should be possible to edit the model to accommodate new devices or test conditions with ease.
  - Interfacing the model with the corresponding controller device I/O should be straightforward.
  - It is compatible with different communications protocols, allowing for complete emulation of real devices.
- Easy-to-use, real-time supervisory environment
  - An easy-to-use real-time interface with the HIL simulator is necessary to both excite the system and to capture and evaluate the signals.
- Test automation platform for repeatable, scalable, and maintainable tests
  - The number of scenarios that a system must be tested against is always growing, as are the number of parameters and configurations for each device. A system must be tested several times while it is configured and parametrized.
  - It is impossible to repeatedly, reliably, and efficiently test all necessary test cases manually, hence the need for test automation, in which it is possible to reproduce the same test procedure over and over, capture and evaluate the response of the system, and automatically generate a useful report.

V. Real-Time Simulation, Control, and Validation Testing

As previously discussed, CHIL provides high fidelity in modeling by removing uncertainty in the control algorithms of asset controls while reducing cost by avoiding asset damage and required equipment. For the scope of this paper, we focus on a single use case that shows a variety of potential applications. The testing engineers created a CHIL configuration that consisted of an inverter controller, a protective relay, an automation controller, and the power system simulator.

The inverter controller is the exact same controller that is used in the inverter hardware. It implements the different communications protocols needed to configure, monitor, and control the inverter operation.

The protective relay is the main protection and control (P&C) device of the installation. This device provides a front panel with pushbuttons and touch display that allows the user to manually operate the inverter in the installation site. Moreover, it is implementing the actual frequency and VAR control of the inverter by dispatching the set points to the inverter controller. For example, when a system fault is detected for a short circuit, the protective relay issues a trip through its output contacts that are wired to the simulator, making the simulation a closed loop.

The automation controller is available for additional control functionality (like a black-start sequence) but is also used as a gateway for the different protocols that inverter controllers can implement.

The simulator combines the interface software and appropriate hardware to run the simulation. The hardware should be able to monitor the external inputs (binary inputs from the protective relay, for example, and the switching signals from the inverter controller) and use those as inputs to a power system model that is being simulated with a small time step. It is a closed-loop simulation, and the results from the simulation are voltage and current signals that are sent back to the inverter controller and the protective relay. Fig. 13 illustrates the closed-loop setup.

By integrating these devices, the engineering team was able to ascertain real switching behavior in a safe testing environment, determine optimal protection settings, verify communications with working equipment, and test difficult load conditions in proposed system configurations.

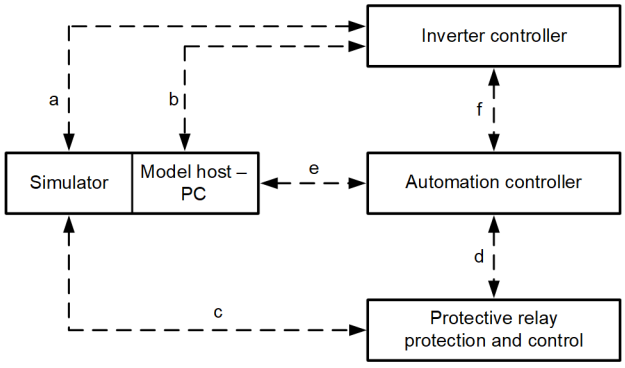

Fig. 13. Test setup.

Fig. 13 illustrates the block interfaces between the hardware used in the testing. The four components shown in the figure need the following interfaces.

One interface (a) corresponds to the switching signals coming from the inverter controller hardware that drive the simulated power electronic switches in the simulator. This interface accommodates the fast switching signals coming from the controller that are being sampled at a high rate to properly model the operation of the full inverter bridge. The appropriate measurements of voltages and currents are sent through low-level signals from the simulator to the inverter controller.

Interface b corresponds to a communications channel that can be used to monitor, manage, and control the inverter. The inverter software that is used to manage settings, monitor measurements, and start and stop the inverter can run in the same environment as the simulator software. In the case of this particular setup, the interface was implemented via CAN bus.

Interface c links the protective relay to the simulator. The protective relay is the P&C device for the installation. It interfaces to the simulator via binary (digital) I/O and analog inputs (voltages and currents). The binary outputs signal the simulator to perform a binary operation (like opening or closing a power system breaker). The binary inputs from the simulator are statuses (of breakers, for example) that the protective relay uses to identify the inverter's mode of operation. Moreover, the voltages and currents that the protective relay requires are provided through this interface.

Interface d allows the exchange of information between the protective relays and the automation controller, which is mainly using the native relay protocols (IEC 61850 and IEEE 37.118) to exchange information. The status of the inverter and measurements are sent to the protective relay. The automation controller sends set points and binary statuses for control.

Interface e links the automation controller and the host PC. The automation controller is a gateway that implements protocols that the simulator and inverter controller understand. Monitoring and status information are exchanged between the simulator and automation controller in this interface.

Interface f links the automation controller to the inverter controller. The set points and other parameters for the operation of the inverter are exchanged in this interface.

A. Tests Performed

The goal of the testing was to verify inverter functionality and controls in a variety of system conditions, as well as experience the CHIL scheme. The model configuration can be seen in Fig. 14. In the example provided, the model can be placed against a stiff utility equivalent network, another real inverter controller in the loop, a generator of approximately equal size, load acceptance and rejection events of different types and sizes (resistive, capacitive, inductive, motor, and constant power), transformer inrush, and every type of fault in varying impedances and durations. A Modbus interface generated inside the HIL can also provide a means to automate the testing process, should a large data sample be necessary.

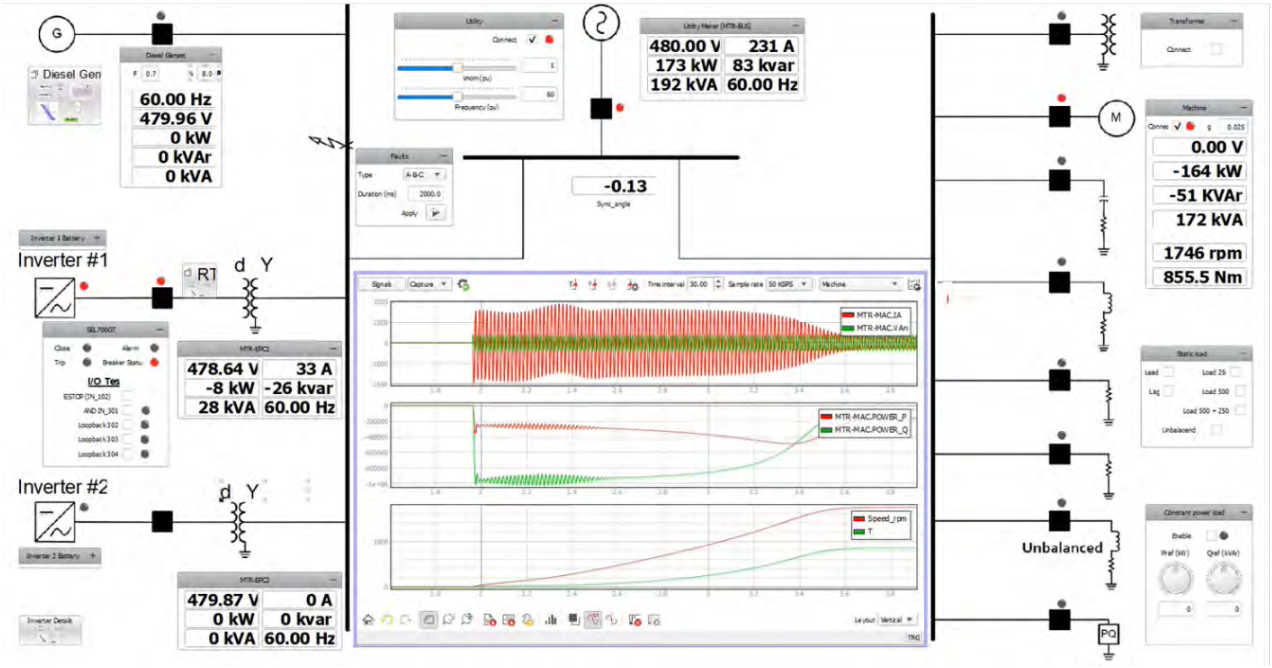

Fig. 14. HIL interface.

B. *Inverter Characteristics*

The intent of the testing in question was to validate behavior in a microgrid application, and thus the inverter configuration reflected this intent. The battery inverter was configured to be 500 kW, operate in GFMD mode, integrate with the third-party logic controller via its Modbus interface, and have a fast ramp rate. The size of 500 kW was chosen as an appropriate representation of inverters for simple commercial and industrial microgrids. GFMD has multiple benefits detailed previously in this paper, and two of the most critical benefits are a seamless transition from grid-tied to islanded conditions and a reduction in load acceptance perceived by the slower synchronous generator provided in the model. The Modbus interface allows the users to configure and dispatch the inverter as it would be in the field, which is useful for fine-tuning the controls prior to commissioning. An example of the desired behavior can be seen in Fig. 15, in which the battery inverter pulls the load in a large load acceptance before slowly offloading to a similarly sized modeled diesel genset.

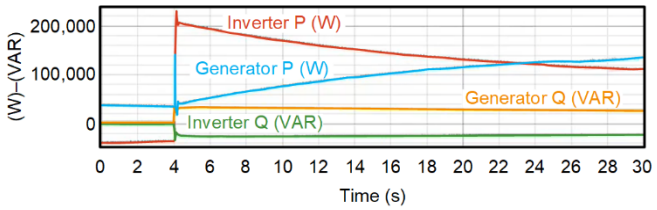

Fig. 15. Modeled IBR and generator load sharing.

The protective relay was used primarily for metering and high fidelity oscillography during trip events from the inverter to provide additional insight into problem areas. Protection functions were disabled during initial testing to better observe the inverter's response characteristics.

One example of how the CHIL test bed allowed for verification of inverter characteristics is through the testing of the configured (P-frequency) droop curve. For this application, the droop settings were configured to be linear in the desired operation region, but to prioritize reactive power. The result can be seen in Fig. 16. When paralleling the inverter with a stiff utility of varying frequency, the active power contribution changes linearly until the limits of the inverter are reached. At that point, active power is curtailed to prioritize VAR contribution per the settings defined in the firmware of the inverter controller.

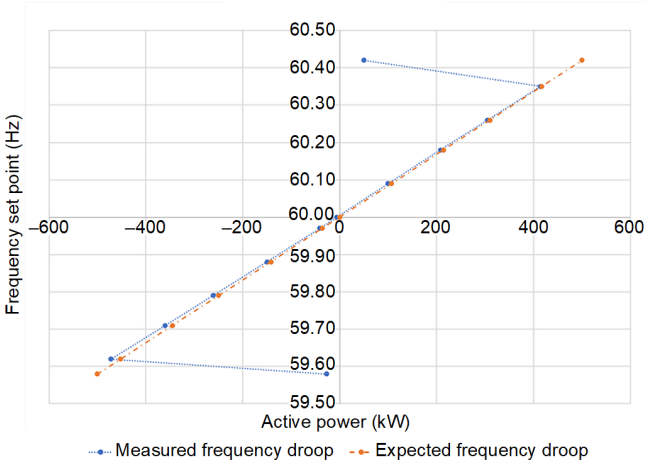

Fig. 16. Inverter frequency droop characteristics. (Note: Power direction is inverted.)

C. *Load Acceptance and Rejection*

Load acceptance can be a challenge for any distributed energy resource (DER), but the challenges may vary by type. For reciprocating engines, the challenge lies in the incremental reserve margin (IRM). DERs of that type may have a large

percentage of their capacity unused, but their ability to maintain stability and responsible emissions requires that only a fraction of that capacity be immediately available for a load acceptance [19]. Similarly, a large load rejection can cause destabilization or unintended operations due to overfrequency events. Inverters can react very quickly to handle these events in contrast to generators that respond on inertia and the available IRM. All available capacity of the inverter can be immediately available. The challenge that inverters face instead is with the different types of loads.

For the purpose of validating the inverter behavior on this system, the model provides examples of transformer and motor inrush, resistive-inductive (RL) loads, and constant power loads. Load acceptance and rejection tests are performed both individually on the inverter and in parallel with a second inverter, a modeled synchronous generator, and a stiff voltage source representing a utility. Configuring the model and paralleling the inverter in the loop already provides some benefits to the user, namely verifying communications, basic dispatch and control of the equipment, and a useful training tool to acquaint users to the interfaces seen in the field in a safe operating environment. The tests that provide the most insight for an inverter, however, are overload and inrush events that cannot be easily replicated on operating equipment.

Fig. 17 shows the load acceptance of a large constant RL load. The test is performed with the GFMD inverter parallel to the modeled stiff utility before opening the utility breaker. The inverter is able to respond in its current configuration by immediately providing its maximum current and curtailing voltage to within its allowable performance band. For RL loads, this allows it to functionally reduce the perceived load in islanded conditions or reduce its contribution while in parallel with other DERs. Understanding this behavior in a modeled environment allows users unfamiliar with their inverters to define the operational scope of their devices and design P&C schemes appropriately prior to field implementation.

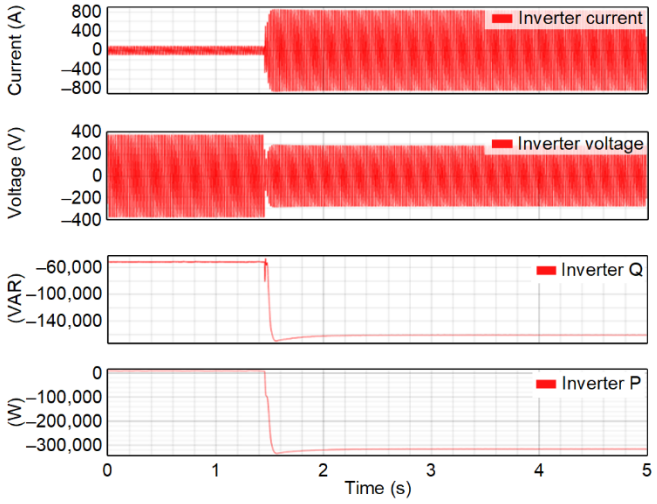

Fig. 17. RL load acceptance is 566 kW and 322 kVAR at nominal voltage. The Inverter P and Q measurements are inverted.

RL loads are not, however, the greatest challenges that inverters face today. Instead, inverters are most challenged by large inrush currents from motors and transformers or by constant power loads, which exhibit behavior opposite of that of the RL loads. Motor loads and transformers pose the same basic problem for inverters. High current inrush events strain the thermal limits of the equipment, so loads need to either be energized over longer periods of time with the same current or the voltage needs to be ramped to avoid the inrush altogether. A successful transformer energization, of a unit equal in size to the IBR, can be seen in Fig. 18. Transformer energization may be too complicated for the inverter to handle, especially if the transformer is bigger than the IBR. In some cases, it may not be possible for a similarly sized transformer to energize from the inverter.

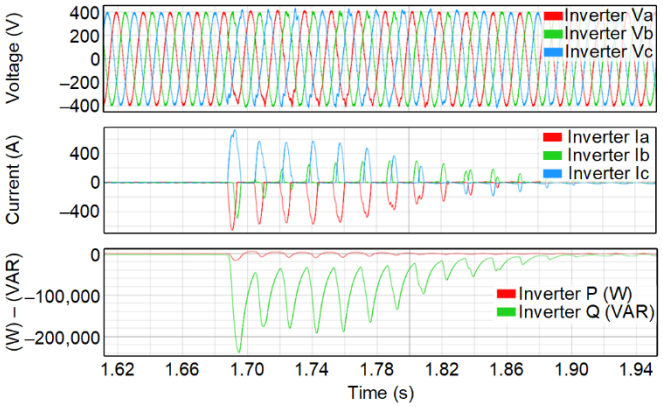

Fig. 18. Successful transformer inrush event.

Motor load energization can be seen in Fig. 19. CHIL provides a convenient way to test the energization events in our system. A modeled fan of 75 kW can prove a challenge, taking 20 seconds to reach full speed. A similar energization against a utility takes only a few seconds, showing the benefit of understanding and testing the current available on systems early in the design process.

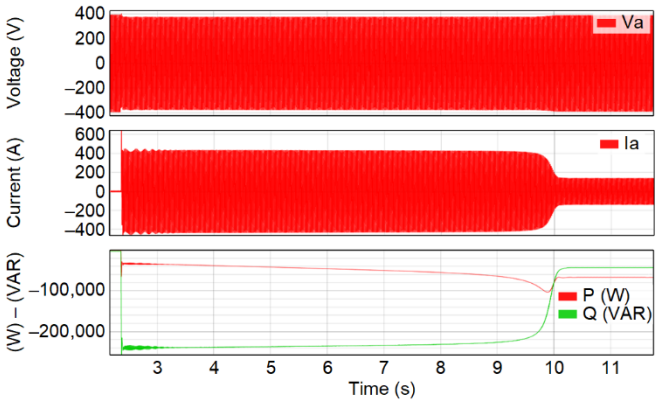

Fig. 19. 75 kW motor load energization.

The last challenge addressed during testing is that of a fully constant PQ load connected to the inverter [20]. When overloaded, a constant PQ load destabilizes an inverter that seeks to limit its contribution by pulling more current as the voltage is curtailed. This behavior can be seen in Fig. 20. Being aware of this behavior in advance allows the user to better define system components, scope of operation, and protection settings before this becomes an issue.

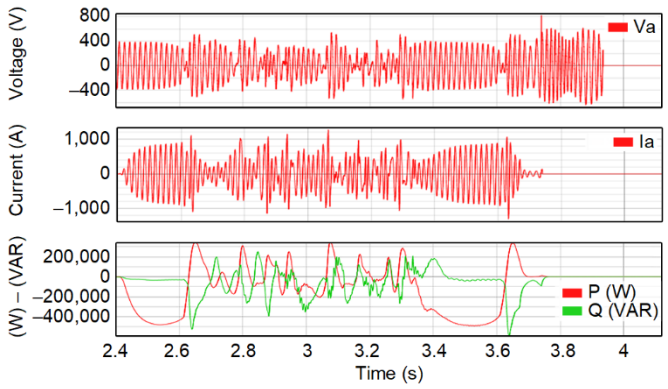

Fig. 20. Switching on a constant P overload from no load.

Fig. 20 illustrates behavior that needs to be considered when energizing constant P or Q loads. Switching power electronic loads or loads where the torque is roughly proportional with speed are examples of constant power loads [20]. Load acceptance is decidedly difficult for inverters and can be evaluated with a CHIL simulation, as shown in the figure. Certainly, the simulation illustrates that an overload of constant P is not acceptable and should be necessary to evaluate smaller values of load to be picked up by the inverter.

D. Fault Behavior

The fault behavior and contributions are also great candidates for CHIL testing. The fault behavior of inverters is a topic of great discussion. CHIL testing faithfully demonstrates the inverter capabilities to provide fault current. The nature of the fault current for the different types of possible faults can be visualized and evaluated. Fig. 21 and Fig. 22 are representative examples of a large number of fault simulations performed with the CHIL setup.

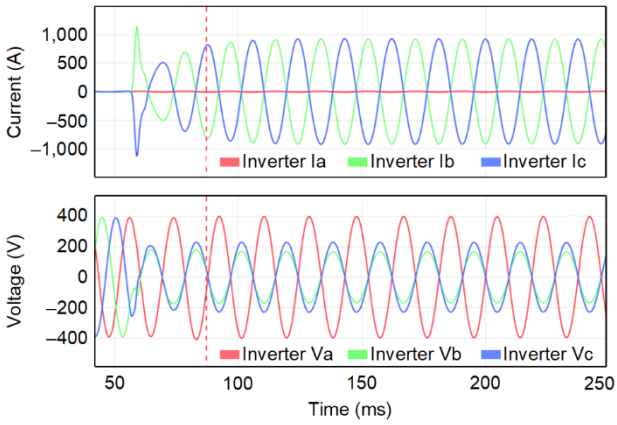

Fig. 21. C-phase-to-ground fault on the high side (wye) of the transformer.

Fig. 21 illustrates a ground fault on the high side of the step-up transformer. On the low side, connected in delta, the fault is effectively a phase-to-phase fault, and no zero-sequence component is possible. The unbalance shown in the figure illustrates clearly that I1 equals I2, as expected for a phase-to-phase fault. The BESS that was tested is capable of producing negative-sequence current to feed the unbalance since it is in GFMD. The possibility of BESS supplying I2 for faults in the power system can be used to propose protective relaying schemes as described in [5].

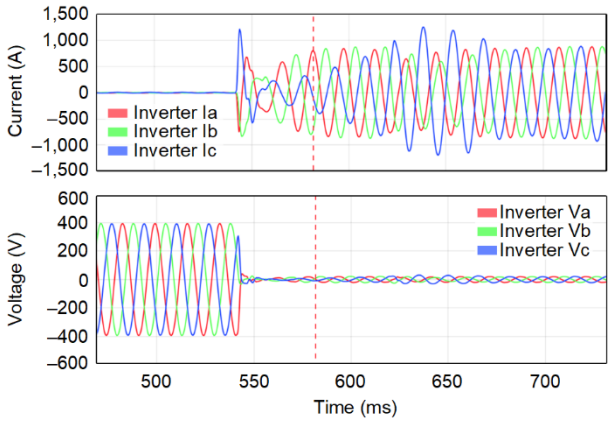

Fig. 22. ABC fault on the high side of the step-up transformer.

Fig. 22 illustrates a three-phase fault on the high side of the transformer. After a while (around 10 cycles), the three phases are balanced and at 1.1 pu. The very first few cycles illustrate the internal transients and time constants for the controller to stabilize the contribution to the three-phase fault. The limited contribution to three-phase faults of inverters needs to be considered when proposing relaying schemes for grid-islanded power systems, as described in [5].

The CHIL simulation can provide valuable information for more complex relaying principles in the power system, like distance or directional protection. The behavior is expected in the field since the inverter controller is the one determining the fault behavior, as illustrated in Fig. 21 and Fig. 22.

VI. Conclusion

The use of a power system simulator, together with the controller hardware (CHIL) and P&C devices for testing, provides meaningful information. The results of the simulations are of greater fidelity compared to simulations where all the components are simulated in software. The simulator should preferably be able to interface to the inverter controller through the controller's switching signals; therefore, it requires a simulator hardware that can scan these signals reliably and with small time steps accommodating the switching frequencies.

The CHIL allows for use of the same communications protocols that the site installation uses. The interface to the devices can be easily tested and perfected with the simulation.

CHIL simulations require less investment in trying to model the controller of the inverter, and the results have greater fidelity and provide greater confidence in the equipment that is going to be installed in the field. Moreover, CHIL is certainly

less costly, safer, and less time-consuming to set up than testing a whole inverter setup, including the power stage.

The CHIL allows for the testing of BESS inverter characteristics, load sharing, load acceptance or rejection, and fault characteristics. CHIL can easily be used to simulate the operation of IBR in the field and add other types of IBRs, such as renewable energy resources, EV fast chargers, VAR compensators, and active filters.

The GFMD is a preferred mode of operation that shows a seamless transition of an IBR microgrid between grid-connected and grid-islanded modes. It allows for simple load sharing with other inverters or DERs, and traditional frequency schemes can be applied.

VII. References

[1] North American Electric Reliability Corporation, "Odessa Disturbance: Texas Events: May 9, 2021 and June 26, 2021 Joint NERC and Texas RE Staff Report," September 2021. Available: nerc.com/pa/rrm/ea/Documents/Odessa_Disturbance_Report.pdf.

[2] North American Electric Reliability Corporation, "1,200 MW Fault Induced Solar Photovoltaic Resource Interruption Disturbance Report: Southern California 8/16/2016 Event," June 2017. Available: nerc.com/pa/rrm/ea/1200_MW_Fault_Induced_Solar_Photovoltaic_Resource_/1200_MW_Fault_Induced_Solar_Photovoltaic_Resource_Interruption_Final.pdf.

[3] North American Electric Reliability Corporation, "900 MW Fault Induced Solar Photovoltaic Resource Interruption Disturbance Report: Southern California Event: October 9, 2017 Joint NERC and WECC Staff Report," February 2018. Available: nerc.com/pa/rrm/ea/October%209%202017%20Canyon%202%20Fire%20Disturbance%20Report/900%20MW%20Solar%20Photovoltaic%20Resource%20Interruption%20Disturbance%20Report.pdf.

[4] North American Electric Reliability Corporation, "San Fernando Disturbance: Southern California Event: July 7, 2020 Joint NERC and WECC Staff Report," November 2020. Available: nerc.com/pa/rrm/ea/Documents/San_Fernando_Disturbance_Report.pdf.

[5] R. Ruppert, R. Schlake, S. Manson, F. Calero, and A. Kokkinis, "Inverter-Based Radial Distribution System and Associated Protective Relaying," proceedings of the 48th Annual Western Protective Relay Conference, Spokane, WA, October 2021.

[6] W. Du, R. H. Lasseter, and A. S. Khalsa, "Survivability of Autonomous Microgrid During Overload Events," *IEEE Transactions on Smart Grid*, Vol. 10, Issue 4, July 2019, pp. 3,515–3,524.

[7] D. Pattabiraman, R. H. Lasseter, and T. M. Jahns, "Comparison of Grid Following and Grid Forming Control for a High Inverter Penetration Power System," *2018 IEEE Power & Energy Society General Meeting (PESGM)*, August 2018, pp.1–5.

[8] C. Michael Hoff, *Energy Storage Architecture*. Elements in Grid Energy Storage, Cambridge University Press, Cambridge, 2022.

[9] H. Magnago, H. Figueira, O. Gagrica, and D. Majstorovic, "HIL-Based Certification for Converter Controllers: Advantages, Challenges and Outlooks," proceedings of the 21st International Symposium on Power Electronics (Ee) 2021, Novi Sad, Serbia, October 2021.

[10] Y. Lin, J. H. Eto, B. B. Johnson, J. D. Flicker, R. H. Lasseter, H. N. Villegas Pico, G. Seo, B. J. Pierre, and A. Ellis, "Research Roadmap on Grid-Forming Inverters," *National Renewable Energy Laboratory*, November 2020. Available: nrel.gov/docs/fy21osti/73476.pdf.

[11] J. Xu, H. Qian, S. Bian, Y. Hu, and S. Xie, "Comparative Study of Single-Phase Phase-Locked Loops for Grid-Connected Inverters Under Non-Ideal Grid Conditions," *CSEE Journal of Power and Energy Systems*, Vol. 8, Issue 1, January 2022, pp. 155–164.

[12] Q. Liu, T. Caldognetto, and S. Buso, "Review and Comparison of Grid-Tied Inverter Controllers in Microgrids," *IEEE Transactions on Power Electronics*, Vol. 35, Issue 7, July 2020, pp. 7,624–7,639.

[13] Y. P. Siwakoti, F. Z. Peng, F. Blaabjerg, P. C. Loh, G. E. Town, and S. Yang, "Impedance-Source Networks for Electric Power Conversion Part II: Review of Control and Modulation Techniques," *IEEE Transactions on Power Electronics*, Vol. 30, Issue 4, April 2015, pp. 1,887–1,906.

[14] W. Du, Q. Jiang, M. J. Erickson, and R. H. Lasseter, "Voltage-Source Control of PV Inverter in a CERTS Microgrid," *IEEE Transactions on Power Delivery*, Vol. 29, Issue 4, August 2014, pp. 1,726–1,734.

[15] Z. Zhou, W. Wang, T. Lan, and G. M. Huang, "Dynamic Performance Evaluation of Grid-Following and Grid-Forming Inverters for Frequency Support in Low Inertia Transmission Grids," *2021 IEEE PES Innovative Smart Grid Technologies Europe (ISGT Europe)*, October 2021, pp. 1–5.

[16] W. Edwards and S. Manson, "Using Protective Relays for Microgrid Controls," proceedings of the 44th Annual Western Protective Relay Conference, Spokane, WA, October 2017.

[17] R. H. Lasseter, J. H. Eto, B. Schenkman, J. Stevens, H. Vollkommer, D. Klapp, E. Linton, H. Hurtado, and J. Roy, "CERTS Microgrid Laboratory Test Bed," *IEEE Transactions on Power Delivery*, Vol. 26, Issue 1, January 2011, pp. 325–332.

[18] D. B. Rathnayake, M. Akrami, C. Phurailatpam, S. P. Me, S. Hadavi, G. Jayasinghe, S. Zabihi, and B. Bahrani, "Grid Forming Inverter Modeling, Control, and Applications," *IEEE Access*, Vol. 9, 2021, pp. 114,781–114,807.

[19] M. M. Al-Mulla and N. C. Seeley, "Distributed Generation Control in Islanded Industrial Facilities: A Case Study in Power Management Systems," proceedings of the PCIC Europe Conference, Oslo, Norway, June 2010.

[20] A. B. Jusoh, "The Instability Effect of Constant Power Loads," *National Power and Energy Conference (PECon) 2004 Proceedings*, November 2004, pp. 175–179.

VIII. Biographies

Henrique Magnago received his control and automation engineering graduate degree (2017) and his master's degree (2019) in power electronics and control from Universidade Federal de Santa Maria (UFSM). Since then, he has been working with Typhoon HIL, Inc. as a test automation engineer, engaging with several customers to improve their test coverage and test automation processes.

Matt Baker is the vice president for grid modernization at Typhoon HIL, Inc. After receiving a BS from the U.S. Naval Academy and an MS from the University of Maryland in aerospace engineering, Matt commenced a 28-year career as an infantry officer for the United States Marines Corps. Upon retiring in 2015, Matt worked at Fairlead Integrated (Earl Energy) with a focus on hybrid power applications. In 2017, he joined Typhoon HIL, where his focus is to provide integrators with model-based systems engineering solutions for power electronics and digital control systems. Applications for Typhoon HIL's technology include integration of distributed energy resources with stochastic loads and digitally controlled distribution systems.

David Nobles is an electrical engineer at EPC Power Corporation, where he is currently working closely with the Typhoon HIL team to improve the research and development (R&D) cycle by implementing a flexible test framework built around the Typhoon HIL system. Previously, he has assisted with certification testing, commissioned engineering, procurement, and construction (EPC) inverters, and contributed to system-level battery energy storage system (BESS) designs for many customers.

Matt Aubuchon joined EPC Power Corporation in 2019 as a power electronics engineer and is currently the director of engineering in San Diego. Prior to EPC, he worked in research and development (R&D) teams at Arrivo, General Atomics, and Sandia National Laboratories. He received BSEE and MSEE degrees from the University of Missouri and is a registered professional engineer in the state of California.

Eric Herman joined EPC Power Corporation in 2021 as director of special projects. Prior to EPC, he was the director of engineering at Mission Critical Electronics, LLC., designing inverters and chargers for the mobile vehicle market. Eric has over 25 years of experience in the power generation industry and received a BSEE degree from The Ohio State University.

Scott Manson received his MSEE from the University of Wisconsin–Madison and his BSEE from Washington State University. Scott is a fellow engineer at Schweitzer Engineering Laboratories, Inc. (SEL). Scott is a registered professional engineer in 6 states and holds 24 patents. Scott can be reached at scott_manson@selinc.com.

Lukas Cevetello received his BSEE from Washington State University in 2019. Since then, he has joined Schweitzer Engineering Laboratories, Inc. (SEL) in the SEL Engineering Services, Inc. (SEL ES) division as a project engineer. His work focuses on the testing and implementation of microgrid systems using controller hardware-in-the-loop simulations, as well as customer outreach via demonstration trailers.

Fernando Calero is a principal engineer at Schweitzer Engineering Laboratories, Inc. (SEL) in the research and development (R&D) division. For many years, he was an application engineer in the SEL international organization. In 2020, he transferred to R&D and is currently working on projects related to renewable sources, protection, and control. He is a registered PE in the state of Florida.